Title

Centrifuge modling of culvert structures to evaluate seismic earth pressures arising from soil-structure interaction.

Authors

Agapaki, Eva
Esmaeilzadeh Seylabi, Elnaz
Brandenberg, Scott J
et al.

Publication Date

2016-06-01

Peer reviewed

ICONHIC 2016
1st International Conference on Natural Hazards & Infrastructure
28-30 June, 2016, Chania, Greece

Centrifuge modeling of culvert structures to evaluate seismic earth pressures arising from soil-structure interaction

E. Agapaki[1], E. Esmaeilzadeh Seylabi, S. J. Brandenberg, J. P. Stewart, E. Taciroglu
University of California, Los Angeles

D. Pitilakis
Aristotle University of Thessaloniki

ABSTRACT

The seismic response of underground structures is a complex soil-structure interaction (SSI) problem in which two fundamental mechanisms are at play—kinematic and inertial interaction. The kinematic component is generally considered to be more significant for seismic response of embedded structures that are not attached to above-ground (super-) structures. We recently conducted a centrifuge modeling test containing two culverts (circular and rectangular) fully embedded within dry Ottawa sand. The tests were performed using a flexible shear beam container so that boundary conditions are generally compatible with free-field conditions for vertically propagating shear waves, and the soil and structures were heavily instrumented. A crucial soil parameter for SSI analysis is the shear wave velocity of the soil (V_S), and its relation with mean effective stress (p'). This paper presents bender element measurements performed at various positions within the model, including in the free-field and beneath the culverts. Signal processing and a cross-correlation procedure are adopted for computing travel times. Mean effective stresses at the bender element array locations are computed using a finite element solution. Arching beneath the culvert structures is demonstrated to be an important aspect influencing p'. The resulting V_S-p' data are regressed using three different functional forms, and a relationship for the dry Ottawa sand is proposed.

Keywords: shear wave velocities, bender elements, cross-correlation, centrifuge experiment, soil-structure interaction

INTRODUCTION

Underground structures have historically experienced less damage than near surface and aboveground structures during earthquakes. However, they have been reported to be severely affected under strong seismic loading (Dowding and Rozen, 1978; Owen and Scholl, 1981; Sharma and Judd, 1991; Power et al., 1998; American Lifeline Alliance, 2001; Corigliano, 2007). A particularly interesting case is the Daikai station in Kobe, Japan, that collapsed during the major Hyogoken-Nambu earthquake in 1995 (Hashash et al., 2001; Asakura and Sato, 1998). Current seismic design practices rely on quasi-static analyses (Mononobe and Matsuo, 1929; NCHRP Report 611, 2008; **C**ulvert **AN**alysis and **De**sign-CANDE 2007) that do not account for the dynamic interaction of the culvert structure with free-field waves and the inertia developed

[1] Corresponding Author: E. Agapaki, *University of California, Los Angeles, agapakieva@gmail.com*

within the culvert structural element. Wang (1993) described soil-structure interaction procedures that can be used in the seismic design of underground structures, followed by Penzien (2000) and Hashash et al. (2001). Pseudo-static methods described in Wang (1993) and Hashash et al. (2001) are very similar to the implementation in CANDE (2007), so these should not be considered distinct methods.

Underground structures undergo three types of deformations when seismically loaded: axial compression/extension, longitudinal bending, and ovaling/racking. The principal factors producing these deformations of culvert structures are spatial variability of ground motions vertically over the height of the culvert section or horizontally over its length (Hashash et al., 2001; Wang, 1993; Brandenberg et al., 2015), permanent displacements of the culvert induced by ground failure (Yoshikawa and Fukuchi, 1984), the relative flexibility of the culvert and soil, and radiation damping (Okamoto 1973; Kawashima, 2000). For the relatively simple case of vertically propagating shear waves, the analytical and numerical methods by Wang (1993), Penzien (2000), and Hashash et al. (2001) can produce significantly divergent predictions in some cases (Fele, 2004).

Relatively few testing campaigns have been undertaken to provide data sets suitable for validation purposes - Pitilakis and Tsinidis (2012) and Lanzano et al. (2012) tested circular culvert sections using flexible-wall containers and Abuhajar (2015) tested a rectangular culvert section. We have undertaken a centrifuge modeling program designed to extend the previous test results by (1) applying a wider range of ground motions spanning frequency contents where interaction effects are expected to range from significant to negligible; (2) applying a wider range of shaking amplitudes to investigate variable effects of soil nonlinearity; and (3) deploying a relatively dense instrument configuration to produce detailed culvert section and free-field soil responses. These centrifuge tests were performed using the 9-*m* radius centrifuge at the Center for Geotechnical Modeling (CGM) at UC Davis. Both rectangular and circular culvert sections were used with a dry Ottawa sand backfill. In this paper, the experimental procedure is briefly presented along with some representative experimental results for the shear wave velocity profile of the model. We describe the analysis of shear wave velocities from bender element data and its variation with mean effective stress, including arching effects for soil materials affected by the presence of the culvert structures.

METHODOLOGY

Model Configuration

Centrifuge modeling increases the gravity imposed on a model such that the stress conditions are representative of a much larger prototype. The test focuses on the soil-structure interaction of two culvert specimens intended to model a reinforced concrete box culvert of size 3.66 *m* x 2.44 *m* and a 2.44 *m* diameter corrugated metal pipe. The rectangular and circular sections were modeled using aluminum structures of dimensions 20.3 *cm* x 12.7 *cm* and 12.7 *cm* (outer diameter) respectively. The geometry of the instrumented cross section is shown in Fig. 1.

Pre-test dynamic finite element simulations were performed to help guide the structural instrumentation plan, and to study the structure-to-structure and structure-to-container interactions. Accelerometers were installed inside the specimens in the horizontal and vertical directions as shown in Fig. 1. Strain gauges were installed inside and outside the specimens to measure hoop strains and bending strains at selected locations around the culverts. Thin aluminum sheets were used to seal the ends of the specimens to avoid sand intrusion. Vertical arrays of accelerometers were installed in the soil to characterize the dynamic response of the model. A total of 25 shaking events were applied to this model at 20*g* centrifugal acceleration. The shaking was applied transverse to the culverts' long axes in the north-south direction.

The soil was a fine, uniform, dense dry Ottawa sand placed in 25.4 *mm* thick layers by dry pluviation, and subsequently vibrated and tamped to a relative density of 90% as shown in Fig. 2. This soil conforms to the select granular fill criterion specified by the Caltrans Seismic Design Criteria. A thin 5 *mm* layer of Monterey sand was placed above the model to prevent wind erosion during spinning. As shown in Fig. 3, sensors were placed in six stages at different elevations in the model, including 59 accelerometers, 43 of which were installed in "free-field" soil and the rest inside the specimens as shown in Fig. 1. As illustrated in

Fig. 3, a frame is mounted on top of the container to hold linear potentiometers (LPs), in order to measure soil surface settlements, while two LPs on the east and west upper side of the walls of the specimens were attached to capture the vertical displacement and the possible rocking of the models. All sensors used in the model were connected to a data-acquisition system and data from all sensors were recorded continuously during the test.

For the purpose of this paper, only shear wave velocity profiles are presented, which were measured in-flight at 20*g* using bender elements. Additional data analysis is ongoing as of this writing.

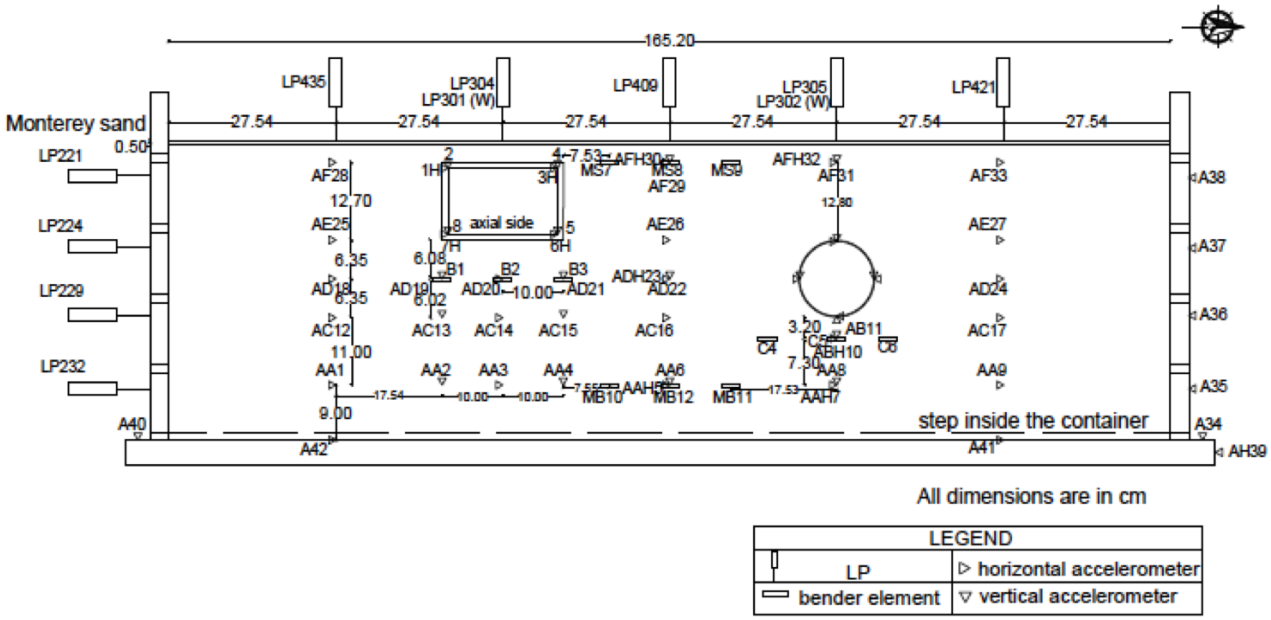

Figure 1. Geometry and instrumentation of centrifuge experiment (model scale)

Bender Element signal processing

Shear wave velocity measurements were obtained at four positions in the soil profile; near the bottom of the container (MB array), below the circular pipe (C array), below the rectangular culvert (B array) and close to the surface of the container (MS array) as shown in Fig. 1 and 3. Center-to-center distance between bender elements is 100 *mm*. In all these arrays, three bender elements are used, which act as piezoelectric transducers, one being the source and the other two being the receivers of the signal. The measurements are taken at 20*g* (during spinning). A high voltage step wave motion is imposed on the source bender element, which causes the element to rapidly bend inducing a horizontally propagating shear wave with vertical particle motion. The wave travels through the soil and deforms the receivers, resulting in a recorded voltage signal.

Shear wave velocity is obtained by measuring the travel time of the wave between two bender elements. The travel time between the two receivers in each elevation was used herein because peripheral sources of phase lag cancel when making receiver-to-receiver measurements, whereas they may cause errors in source-to-receiver measurements (Lee and Santamarina 2005). Obtaining good quality signals in large centrifuge experiments is complicated because mechanical vibrations often have larger amplitudes than the shear waves generated by the bender elements. These vibrations are reduced by digital filtering and signal stacking to improve signal-to-noise ratio (Brandenberg et al., 2006), and occur predominantly at frequencies lower than the bender element signals. Three different basic approaches have been identified for determining the shear wave travel time: observational techniques of the "start-to-start" and "peak-to-peak" signal in the source and receivers, cross-correlation (CC) of the signals and a cross-power spectrum calculation of the signals (Yamashita et al. 2009). The last two approaches are techniques applied in the time- or frequency-domain. The first technique involves visual selection of travel times, which is often subjective, particularly for source-to-receiver measurements. We apply the second (CC) technique to automate travel time picks; this procedure is described below.

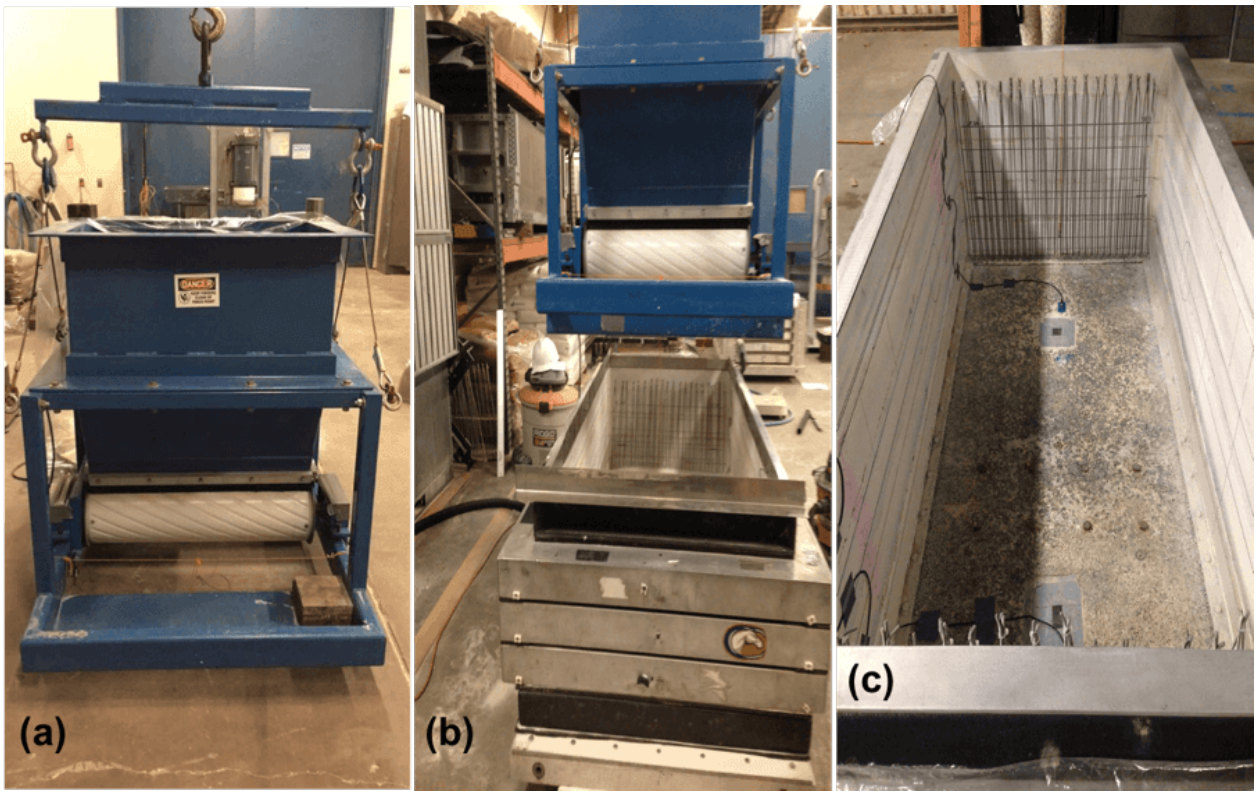

Figure 2. (a) Northern side of the dry sand pluviator, (b) pluviation technique and (c) flexible shear beam container (FSB2), 800 mm wide and 1650 mm long.

Equation 1 provides the continuous cross-correlation function cc_{xy}, with respect to source signal time shift, τ,

$$cc_{xy}(\tau)=\lim_{T\to\infty}\frac{1}{T}\int_{0}^{T}x(\tau)\,y(t+\tau)dt \tag{1}$$

where T corresponds to the signal time record and $y(t)$ and $x(t)$ correspond to the two received signals, respectively. Equation 1 can also be written as an alternative expression of the CC between the two received signals in the frequency domain, which was used in this study,

$$CC_{xy}(f)=X(f)\overline{Y(f)} \tag{2}$$

where $CC_{xy}(f)$, $X(f)$ and $Y(f)$ are the Fourier transforms of $cc_{xy}(\tau)$, $x(t)$ and $y(t)$, respectively, and the bar denotes the complex conjugate. The travel time of the shear wave is defined as the time corresponding to the maximum of CC.

The centrifuge was spun to 20*g* to perform testing, and data were acquired from the bender element arrays. A sample signal of the four arrays and the procedure we used to process it is given in Fig. 4. Fig. 4 (a) shows the recorded signals from the two receiver benders for one of the four element arrays installed in our model for a dataset close to the step function pulse imposed. The signals were truncated to 2^N number of data points, so that a Fast Fourier Transform (FFT) could be performed. Four signals are plotted in Fig. 4 (a), with two signals for each receiver bender element. The source bender element is pulsed with a positive step wave, then with a negative step wave and results for each are shown. High-amplitude, low-frequency noise is superposed on the bender element signals because the centrifuge induces significant vibrations during spinning. Furthermore, the bender element voltages all exhibit a sudden increase when the source is excited due to electrical coupling. To reduce the influence of these factors, the mean of positive and negative signals is computed for each bender element, the initial portion of the signal associated with electrical coupling is truncated, and the signals are baseline corrected by subtracting a seventh order polynomial fit to the signal. The resulting post-processed signals used for cross-correlation are shown in Fig. 4 (c), and the cross-

correlation versus time lag is shown in Fig. 4 (d). The travel time is taken as the time lag associated with the peak of the absolute value of the cross-correlation. It is possible for the negative peak to be larger than the positive peak depending on the orientation of the bender elements, which was not recorded in these experiments.

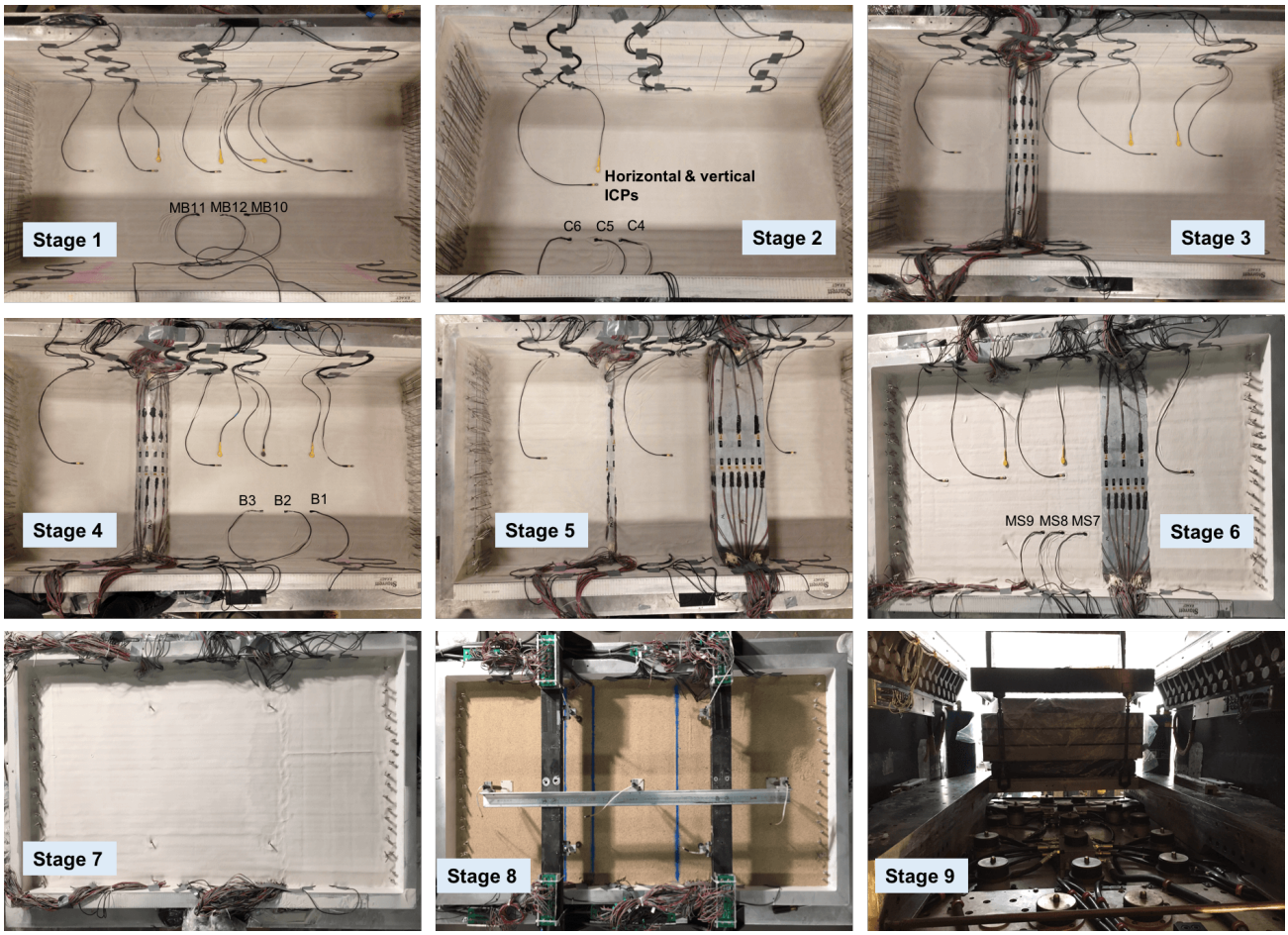

Figure 3. Stages of model construction and layout of sensors at each layer within the shear beam container.

The cross-correlation procedure cannot always produce accurate travel times when the two received signals differ due to wave dispersion, or differences in the responses of the bender elements. For example, travel time for the array of bender elements located below the rectangular box (B array in Fig. 1) was selected visually by observing the "peak-to-peak" travel time because the peak in the cross-correlation signal did not correspond to the correct offset. Furthermore, the shallow free-field bender element array (MS array in Fig. 1) required special attention because the bender elements do not function as well at low confining pressures. In this case, the signals were processed by a cosine taper, and filtered using a high-pass Butterworth filter (Eq. 3) in lieu of baseline correction.

$$H = \frac{1}{\sqrt{1+\left(\frac{f_c}{f}\right)^4}} \tag{3}$$

where f_c is the corner frequency. These cases illustrate that careful review of data quality is needed when interpreting bender element signals.

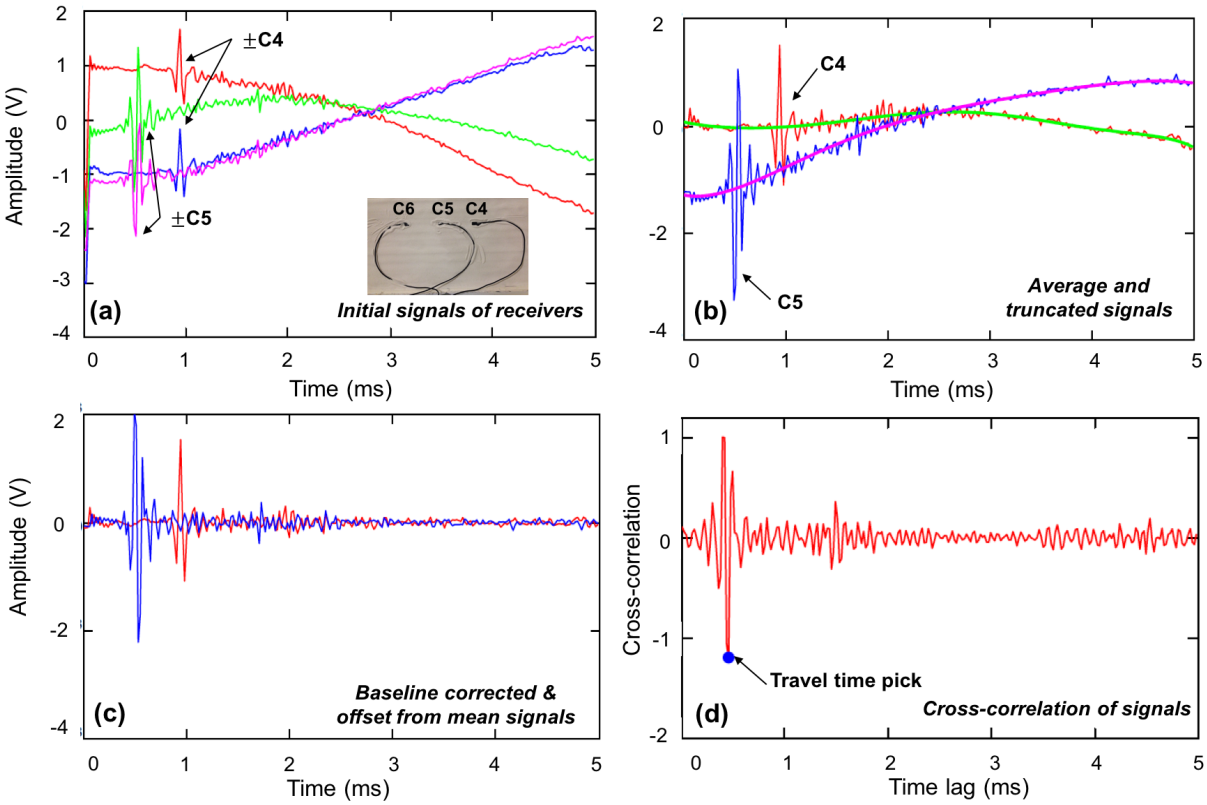

Figure 4. Example procedure to process bender element receivers' data (C4, C5) below the pipe (C-array), (a) unprocessed plus and minus signals, (b) average and truncated signals, (c) post-processed signals and (d) cross-correlation used to find travel time.

Numerical analysis

For one-dimensional problems, vertical stress is often computed as the depth integral of unit weight evaluated from the surface to the point of interest. This procedure is inappropriate for the problem at hand because (1) the open space inside the culverts complicates this calculation, and (2) the culverts cause arching in the surrounding soil that alters the soil stresses. Hence, the mean effective stresses at the position of the bender element arrays were obtained by numerical analysis performed in a finite element program Phase^2 (Rocscience, 2011). A finite element mesh was defined based on 6-node triangular elements. The bottom boundary of the model was fixed while the vertical boundaries were constrained horizontally but free to move vertically to resemble boundary conditions imposed by the model container. The model geometry along with the main dimensions in prototype scale are given in Fig. 5 (a). The problem is studied in prototype "real" scale and not model "experiment" scale, since the shear wave velocity measurements were taken while spinning at 20*g*. The soil has the properties of Ottawa sand deposited using a pluviation technique (D_R=*90 %*, γ=*17 kN/m^3*, *E=200 MPa*) and it was modeled as a linear elastic medium. Both culverts are assigned Aluminum 60-61 properties (γ=*26.5 kN/m^3*, *E=68.9 GPa*). The elastic moduli of the soil are known to depend on mean confining pressure *p'*, but were modeled as constant herein for simplicity.

The mean effective stresses, shown in Fig. 5 (b), were obtained by applying gravity load in the model. Because of stiffness contrasts between the culverts and the surrounding soil, stress concentrations form below the edges of both culverts and significantly reduced stresses in soil below the structures relative to the free-field. This arching effect influences the measurements taken for the receivers in the locations shown in Fig. 5 (b). Observations of soil arching were first reported in dry sand by Terzaghi (1936).

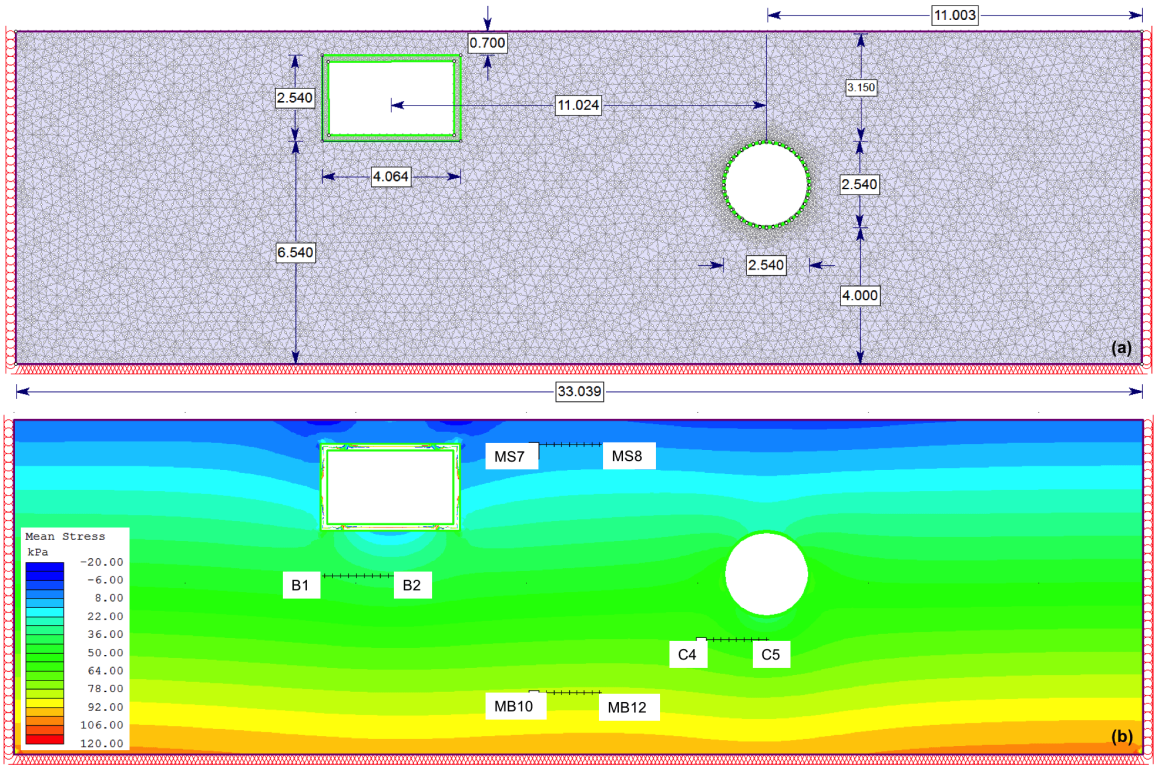

Figure 5. (a) Geometry and finite element model mesh used in numerical analysis, (b) mean effective stress contours and locations of bender element receivers.

RESULTS

Fig. 6 shows the variation of shear wave velocity with normalized mean effective stress. Laboratory testing has shown that the velocity of a propagating shear wave depends on principal effective stresses in the directions of wave propagation and particle motion (Roesler, 1979; Yu and Richart, 1984; Stokoe et al., 1985), which is well represented in an average sense by p'.

The basic functional form used to regress the data is provided in Eq. 4, where $p' = (\sigma'_1 + \sigma'_2 + \sigma'_3)/3$ and p_a is atmospheric pressure in the same units as p', V_{S0} is the value of shear wave velocity at $p' = 0$, and V_{S1} is the shear wave velocity at $p' = p_a$. Three variations were used in the regression. In the first form, V_{S0} was set to 0, and m was set to 0.25, while V_{S1} was regressed. This is consistent with the form suggested by Hardin and Drnevich (1970). In the second form, V_{S0} was set to 0, while m and V_{S1} were regressed. This is consistent with the form suggested by Roesler (1979). Finally, all three variables were regressed to fit the data. This is consistent with the form suggested by Rovithis et al. (2011), though their form was presented in terms of depth rather than effective stress.

$$V_S = V_{S0} + (V_{S1} - V_{S0}) \left(\frac{p'}{p_a}\right)^m \tag{4}$$

The root mean square error was computed for each form, and was smallest for the Rovithis et al. form. Hence, we suggest that this form provides the best representation of the experimental data. Including a non-zero value of V_S at $p' = 0$ is not strictly true for uncemented sands, but this form matches measurements better than the other two for the levels of confinement at the locations of measured velocities.

General guidelines for values of m provided by Lee et al. (2005) and Yamada et al. (2008) are m = 0.16-0.25 for granular soils (increasing with density and decreasing with angularities of sand), which can be compared to values of 0.15-0.3 for silts and clays. The values of m regressed herein are in reasonable agreement with these findings.

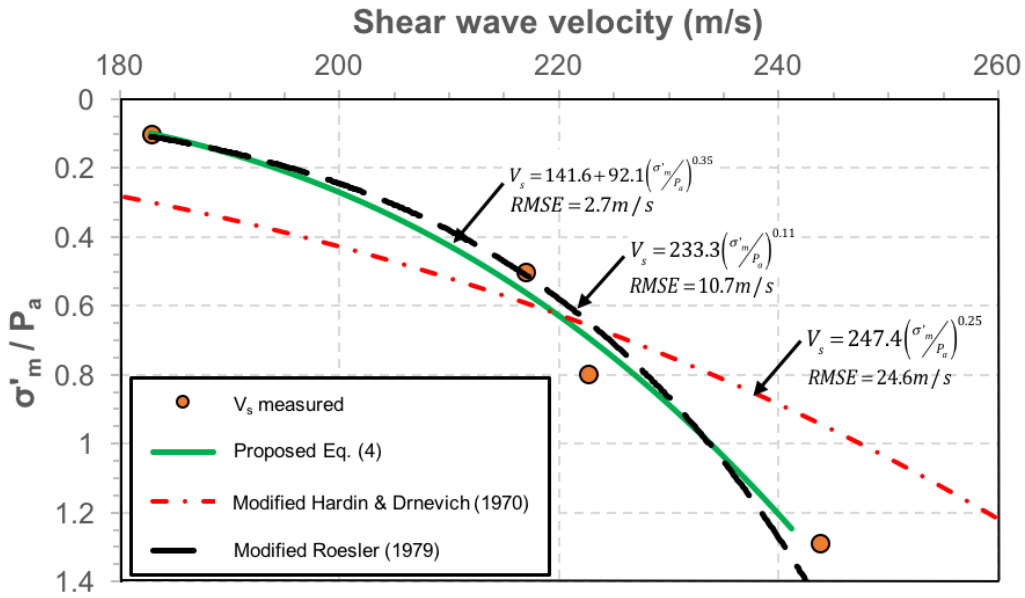

Figure 6. Shear wave velocity measurements with normalized mean effective stresses and fitted prediction equation. The recommended relation is the green curve, which has the lowest RMSE.

CONCLUSIONS

A series of centrifuge tests were carried out to study dynamic SSI for two culverts embedded in sand. Shear wave velocity is an important input parameter for SSI studies, and this paper presented procedures for relating measured values of V_S with computed values of p'. Receiver-to-receiver bender element measurements using cross-correlation or "peak-to-peak" travel time picks were used to measure V_S at various positions in the model. Signal processing was needed to recover high quality signals. Elastic static finite element simulations of the models showed that arching effects near the culverts significantly influenced p' compared with the "free-field". This, in turn, influenced the soil stiffness, which may be of practical interest for underground construction. The relationship between V_S and p' following Rovithis et al. (2011), which includes a non-zero V_S at $p' = 0$, provides a better fit to the data than two other forms. The variation of V_S with p' as found in the present work is reasonably consistent with relationships in the literature.

The recorded dataset provides ample opportunity to investigate the seismic response of culvert structures, which is a complex SSI problem. Future research will study the mobilization of earth pressures along the boundaries of the culvert-soil interface to ascertain the influence of earthquake shaking on structural demands imposed on the culverts. Hoop and bending strains will be used to back-calculate the soil demands. However, these studies are ongoing, and their presentation is reserved for future publications.

ACKNOWLEDGEMENTS

The authors would like to express their great appreciation and thanks to all staff members of the Center for Geotechnical Modeling (CGM) at UC Davis, USA, for providing support during the experiment. The work presented here was funded by the California Department of Transportation (Caltrans), United States. Grant no. 65A0561. Any opinions, findings and conclusions or recommendations expressed in this paper are those of the authors and do not necessarily reflect the views of the Caltrans.

REFERENCES

Abuhajar O., Naggar H.El., Newson T. "Static soil culvert interaction the effect of box culvert geometric configurations and soil properties". *Journal of Computers and Geotechnics*, 69: 219-235, 2015.

American Lifeline Alliance, "Seismic Fragility Formulations for Water Systems", 2001.

Asakura T. and Sato Y. "Mountain Tunnels Damage in the 1995 Hyogoken-Nanbu Earthquake," QR of Railway Technical Research Institute (RTRI), 39(1), 9-16, 1998.

Brandenberg S.J., Choi S., Kutter B.L., Wilson D.W., and Santamarina J.C. A bender element system for measuring shear wave velocities in centrifuge models. *6th International Conference on Physical Modeling in Geotechnics*, 165-170, 2006.

Brandenberg S.J., Mylonakis G., and Stewart J.P. "Kinematic framework for evaluating seismic earth pressures on retaining walls." *Journal of Geotechnical and Geoenvironmental Engineering*, 141:1-10, 2015.

California Department of Transportation. Highway design manual, 2011.

Corigliano, M., Scandella, L., Barla, G., Lai, C. G., Paolucci, R. C. "Seismic analysis of deep tunnels in weak rock: a case study in southern Italy," *4th International Conference on Earthquake Geotechnical Engineering*, Paper No. 1616, Thessaloniki, Greece, 2007.

Dowding, C.H., Rozen A. "Damage to Rock Tunnels from Earthquake Shaking", *Journal of Geotechnical Engineering Division*, ASCE 104 GT2, 175-191, 1978.

Fele, F. "Seismic analysis of the structure of an underground railway station, including SSI", M.S. Thesis, Rose School, *2004*.

Hardin, B.O. and Drnevich V.P. "Shear modulus and damping in soils. Technical report", University of Kentucky, 1970.

Hashash Y.M.A., Hook J.J., Schmidt B., Yao J.I.-C. "Seismic design and analysis of underground structures." *Tunneling Underground Space Technology*, 16 (2), 247-293, 2001.

Kawashima, K."Seismic Design of Underground Structures in Soft Soil Ground: A Review, Key Note Presentation," *Geotechnical Aspects of Underground Construction in Soft Ground, Balkema, Rotterdam*, 3-19, 2000.

Lanzano G., Billota E., Usso G., Silvestri G., and Madabhushi S.P.G. Centrifuge modeling of seismic loading on tunnels in sand, Geotechnical Testing Journal, 35, 2012.

Lee, J.S., and Santamarina, J.C. (2005). "Bender Elements: Performance and Signal Interpretation" *Journal of Geotechnical and Geoenvironmental Engineering,* 131(9), 1063-1070.

Lee, J. S., Fernandez, A. L., and Santamarina, J. C. "S- wave Velocity Tomography: Small-Scale Laboratory Application," *Geotechnical Testing Journal,* Vol. 28, No. 4, 336–344, 2005.

Mononobe, N., and Matsuo, M. "On the determination of earth pressures during earthquakes.", *World Engineering Congress, Engineering Society of Japan, Tokyo*, 179–187, 1929.

NCHRP (National Cooperative Highway Research Program). "Seismic analysis and design of retaining walls, buried structures, slopes, and embankments." Rep. 611, D. G. Anderson, G. R. Martin, I. P. Lam, and J. N. Wang, eds., National Academies, Washington, DC, 2008.

Okamoto, S. "Introduction to Earthquake Engineering", University of Tokyo Press, Tokyo, Japan, 1973.

Owen, G.N. and Scholl, R.E. "Earthquake Engineering of Large Underground Structures." Report no. FHWARD-80-195, *Federal Highway Administration and National Science Foundation*, 1981.

Penzien J. "Seismically induced racking of tunnel linings." *Earthquake Engineering Structural Dynamics*, 29, pp. 683-691, 2000.

Pitilakis K.K., Tsinidis G. "Performance and seismic design of underground structures." *II International Conference on Performance Based Design in Earthquake Geotechnical Engineering*, Taormina, Italy, May, 2012.

Power M., Rosidi D., Kaneshiro J., Gilstrap S., Chiou S.J. "Summary and evaluation of procedures for the seismic design of tunnels." Final Report for Task 112-d-5.3(c). *National Center for Earthquake Engineering Research, Buffalo*, New York, 1998.

Rockscience, Phase^2, Manual, https://www.rocscience.com/help/phase2/webhelp/tutorials/Phase2_Tutorials.htm, 2011.

Roesler, S. K. "Anisotropic shear modulus due to stress anisotropy." *Journal of Geotechnical Engineering*, Vol. 105, No. 7, 871-88, 1979.

Rovithis E., Parashakis H., Mylonakis G. "1D harmonic response of layered inhomogeneous soil: Analytical investigation." *Soil Dynamics and Earthquake Engineering 2011*; 31(7):879–890.

Sharma S. and Judd W.R. "Underground opening damage from earthquake", *Engineering Geology*, Vol. 30: 263-273, 1991.

Stokoe, K. H., II, Lee, S. H. H., and Knox, D. P. "Shear Moduli Measurement under True Triaxial Stresses," *Proceedings of the Geotechnical Engineering Division: Advances in the Art of Testing Soil Under Cyclic Conditions, ASCE,* Detroit, MI, 166-185, 1985.

Terzaghi, K. "Stress Distribution in Dry and in Saturated Sand Above a Yielding Trap-Door", *Proceedings, First International Conference on Soil Mechanics and Foundation Engineering,* Cambridge, Massachusetts, 307-311, 1936.

Wang, J.N. "Seismic Design of Tunnels, A state-of the-Art Approach", Monograph 7, *Parsons Brinckerhoff Quade & Douglas, Inc*., New York, 1993.

Yamada, S., Hyodo, M., Orense, R.P., Dinesh, S.V., and Hyodo, T. (2008). "Strain-dependent dynamic properties of remolded sand-clay mixtures," *J. Geotech. & Geoenviron. Engrg*. ASCE, 134 (7), 972-981.

Yamashita S., Kawaguchi T., Nakata Y., Mikami T., Fujiwara T. and Shibuya S. "Interpretation of international, parallel test on the measurement of Gmax using bender elements." *Soils and Foundations* 49 (4), 6: 31-650, 2009.

Yoshikawa, K., Fukuchi, G. “Earthquake Damage to Railway Tunnels in Japan,” *Advances in Tunneling Technology and Subsurface Use*, Vol.4 Nr.3, 75-83, 1984.
Yu, P. and Richart, F. E. Jr. “Stress ratio effects on shear modulus of dry sands.”, *Journal of Geotechnical Engineering*, Vol. 110, No. 3, 331-345, 1984.